

RSEdit: Text-Guided Image Editing for Remote Sensing

Zhenyuan Chen
bili_sakura@zju.edu.cn
School of Earth Sciences, Zhejiang
University
Hangzhou, China

Zechuan Zhang
zechuan@zju.edu.cn
ReLER, CCAI, Zhejiang University
Hangzhou, China

Feng Zhang
zfcarnation@zju.edu.cn
School of Earth Sciences, Zhejiang
University
Hangzhou, China

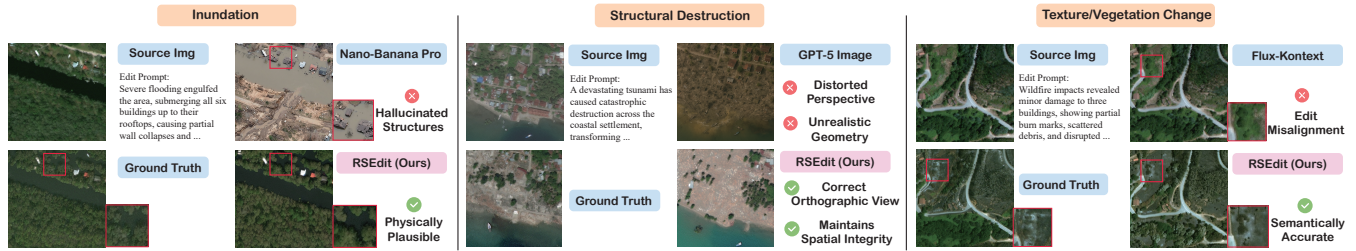


Figure 1: RSEdit enables high-quality, instruction-following editing of remote sensing imagery. Given a source satellite image and a natural language instruction, our framework generates result images that are both physically plausible and faithful to the instructions. This figure showcases the diverse editing capabilities of our model across various scenarios.

Abstract

General-domain text-guided image editors achieve strong photorealism but introduce artifacts, hallucinate objects, and break the orthographic constraints of remote sensing (RS) imagery. We trace this gap to two high-level causes: (i) limited RS world knowledge in pre-trained models, and (ii) conditioning schemes that misalign with the bi-temporal structure and spatial priors of Earth observation data. We present **RSEdit**, a unified framework that adapts pre-trained text-to-image diffusion models—both U-Net and DiT—into instruction-following RS editors via channel concatenation and in-context token concatenation. Trained on over 60,000 semantically rich bi-temporal remote sensing image pairs, **RSEdit** learns precise, physically coherent edits while preserving geospatial content. Experiments show clear gains over general and commercial baselines, demonstrating strong generalizability across diverse scenarios including disaster impacts, urban growth, and seasonal shifts, positioning **RSEdit** as a robust data engine for downstream analysis. Code is available at <https://github.com/Bili-Sakura/RSEdit-Preview>.

Keywords

remote sensing, image editing, text-guided editing, diffusion models

1 Introduction

Text-guided image editing has revolutionized content creation in computer vision, enabling users to modify visual content through intuitive natural language instructions [Cao et al. 2025; Foo et al. 2025; Huang et al. 2025; Zhan et al. 2025]. Recent diffusion-based models have achieved remarkable success in the general domain, allowing for precise photorealistic modifications while preserving

the semantic integrity of the original scene [Brooks et al. 2023; Liu et al. 2025b; Yu et al. 2025a; Zhang et al. 2023a, 2025b; Zhao et al. 2024a]. These advances open a promising avenue for Remote Sensing (RS), where simulating environmental changes—disaster impacts, urban expansion, seasonal shifts—can serve as a powerful data engine for downstream analysis and augmentation [Khanna et al. 2024; Liu et al. 2025a; Tang et al. 2024; Toker et al. 2024]. The utility of RS editing spans diverse applications—disaster simulation [Adriano et al. 2021; Chen et al. 2025b; Wang et al. 2025; Zheng et al. 2025, 2021b, 2024b], urban change modeling [Wang et al. 2024a,c, 2026, 2024b; Xuan et al. 2025], and seasonal dynamics [Christie et al. 2018; Cong et al. 2022; Mañas et al. 2021; Plekhanova et al. 2025; Stewart et al. 2023; Wang et al. 2023].

Modeling disaster events with scarce data is extremely challenging. Relying solely on captured imagery series limits the diversity and redundancy required for training robust analysis models. To address this, we propose a scalable data engine driven by a specialized image editing model, capable of synthesizing disaster event imagery on demand. Given any pre-event satellite image, our system simulates diverse disaster scenarios with free-style yet region-accurate prompts—for instance, transforming a village into a post-flood landscape with controllable damage severity, ranging from minor inundation to complete structural collapse.

Applying general-purpose editing paradigms directly to RS imagery remains challenging. RS images enforce an orthographic viewpoint, strictly defined spatial scales, and complex physical dynamics. General-domain editors often hallucinate non-existent structures or violate gravity when prompted with RS-specific instructions. We attribute this to two root causes: (i) limited RS world knowledge in pre-training, and (ii) conditioning schemes misaligned with the bi-temporal nature and spatial priors of Earth observation data.

To bridge this gap, we introduce **RSEdit**, a universal framework for text-guided RS image editing. Unlike prior methods tied

to specific architectures, **RSEdit** adapts pre-trained text-to-image (T2I) diffusion models into robust editors through architecture-aware conditioning: channel concatenation for U-Net backbones (e.g., Stable Diffusion [Rombach et al. 2022]) and in-context token concatenation for DiT backbones (e.g., PixArt- α [Chen et al. 2024]). **RSEdit** learns precise semantic modifications while preserving geospatial structure.

Our main contributions are threefold: (1) a universal adaptation strategy that converts pre-trained U-Net and DiT diffusion models into instruction-following RS editors via channel and token concatenation; (2) proposal of specialized metrics to measure the editing quality and performance specific to remote sensing image editing, particularly for building damage instruction following by utilizing a pre-trained building damage assessment model; and (3) extensive experiments showing state-of-the-art visual and quantitative performance, including strong generalization to unseen tasks and datasets.

The remainder of this paper is organized as follows. Section 2 reviews related work. Section 3 details the proposed **RSEdit** framework. Section 4 presents experiments. Section 5 concludes the paper with future work.

2 Related Work

2.1 Remote Sensing Image Generation

Recent progress in diffusion models has enabled high-fidelity generation of remote sensing imagery, evolving from unconditional synthesis to sophisticated controllable frameworks.

Metadata/Text Conditional Generation. DiffusionSat [Khanna et al. 2024] pioneers with a U-Net based generative models (fine-tuned on Stable Diffusion [Rombach et al. 2022]) which accepts both metadata and textual description for high-resolution image generation. RSDiff [Sebaq and ElHelw 2024] adopts a two-stage framework similar to SDXL [Podell et al. 2024]. Text2Earth [Liu et al. 2025a] scales the training dataset to 10.5 million image–text pairs with multi-level ground sampling distance image generation capabilities while ZoomLDM [Yellapragada et al. 2025] employs self-supervised learning (SSL) techniques for multi-resolution generation even at 4k resolution. Besides, MetaEarth [Yu et al. 2025b] further adopts a self-cascaded framework [Ho et al. 2022] for any-resolution generation. HSiGene [Pang et al. 2026] extends image generation from RGB domain to hyperspectral domain while Zhang *et al.* [Zhang et al. 2026] builds SAR image generation models.

Image Conditional Generation. To enhance utility, recent works incorporate pixel-level guidance instead of global guidance (i.e. text and metadata). Most commonly, building a conditional image diffusion model from U-Net is to inject auxiliary information into feature maps in each stage. ControlNet [Zhang et al. 2023c] provides a universal strategy to various conditions, which is adopted in CRS-Diff [Tang et al. 2024], TerraGen [Tang et al. 2025], EarthSynth [Pan et al. 2025] and GeoSynth [Sastry et al. 2024]. To further improve high-quality objects layout control, CARD-RS [Zhang et al. 2025a] utilizes cascaded autoregressive models with a decoupled generation strategy for objects. Among the control signals, semantic map is essential in remote sensing interpretation. Given this, specific applications include change detection

data synthesis in Changen [Zheng et al. 2023], Changen2 [Zheng et al. 2024a], ChangeDiff [Zang et al. 2025], Noise2Change [Liu et al. 2025c] TISynth [Dong et al. 2026] and TODSynth [Yang et al. 2025] as temporal semantic change detection data generators. The pre-trained models synthesize datasets hybrid with real ones to improve downstream task performance including object detection, image scene classification and semantic segmentation. Specifically, SatSyn [Toker et al. 2024], instead taking it as a conditional image generation task, introduces a method to generate image-mask pairs through modeling joint distribution of image and masks simultaneously. While these methods offer spatial control via masks or layouts, they focus primarily on synthesizing new images from scratch rather than precise editing of existing imagery, limiting their ability to perform instruction-based semantic modification on real-world images.

2.2 Remote Sensing Image Editing

Image editing is defined as modifying the appearance, structure, or content of an existing image to achieve a desired outcome guided by prompts [Huang et al. 2025]. General-domain editing has flourished with both training-free methods [Meng et al. 2022; Mokady et al. 2023] and training-based approaches [Brooks et al. 2023; Yu et al. 2025a; Zhang et al. 2023b; Zhao et al. 2024b]. The latter, such as InstructPix2Pix, typically achieve superior performance by learning from large-scale paired data. In contrast, remote sensing editing remains under-explored. Early attempts like Han *et al.* [Han et al. 2025] rely on complex and constrained architectures, limiting their capabilities to simple object-level addition or removal. ChangeBridge [Zhao et al. 2025] introduced ChangeBridge, a multi-task framework incorporating segmentation maps and layouts; however, its broad focus limits its effectiveness for pure text-guided editing, specifically failing to handle long, semantically rich prompts and complex structural changes. Crucially, existing methods often fail to handle the complex, semantically rich changes unique to Earth observation and do not scale well to diverse architectural backbones. To our knowledge, no prior work has systematically validated text-guided editing across both U-Net and DiT diffusion architectures in remote sensing, a gap this work aims to fill.

3 Methods

3.1 Preliminaries

We formulate text-guided remote sensing image editing as a conditional generation problem. Given a source satellite image $I \in \mathbb{R}^{H \times W \times 3}$ and a text instruction T describing the desired semantic change (e.g., “flood the coastal area”), the goal is to generate an edited image $I' \in \mathbb{R}^{H \times W \times 3}$ that follows the instruction while preserving the spatial structure and unedited content of I .

We operate within the latent diffusion framework [Ho et al. 2020; Rombach et al. 2022]. The model learns to denoise a latent code $z_t \in \mathbb{R}^{h \times w \times d_z}$ at timestep t conditioned on a text embedding $c_T \in \mathbb{R}^{d_T}$ and an image condition c_I . The simplified training objective is:

$$\mathcal{L} = \mathbb{E}_{z_0, t, \epsilon, I, T} \left[\|\epsilon - \epsilon_\theta(z_t, t, c_T, c_I)\|_2^2 \right], \quad (1)$$

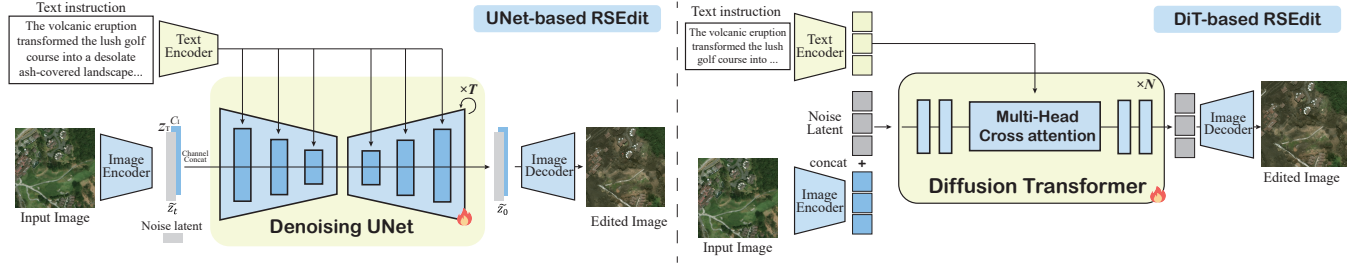


Figure 2: Overview of the RSEdit framework. We propose a universal adaptation strategy that aligns the conditioning mechanism with the architecture’s inductive bias. For U-Net backbones (left), we use channel concatenation to leverage convolutional priors. For DiT backbones (right), we use token concatenation to exploit the in-context learning capabilities of transformers.

where c_t is the conditioning derived from the source image I . The core challenge lies in designing c_t to align with the inductive bias of different backbones.

3.2 Universal Adaptation Strategy

While text-guided editing has matured in general computer vision, directly applying these frameworks to remote sensing (RS) reveals a critical bottleneck: existing methods are often heavily optimized for specific architectures, lacking the flexibility to adapt to the diverse backbones required for RS tasks. We argue that a robust RS editor must not be architecture-agnostic, but rather *architecture-aware*. We observe that the efficacy of the conditioning signal—the source image—depends intrinsically on the *inductive bias* of the underlying diffusion backbone. Consequently, RSEdit proposes a unified yet adaptive framework that tailors the conditioning mechanism c_t to respect the distinct processing paradigms of multi-level style (i.e. U-Net) and sequence modeling style (i.e. DiTs).

Convolutional Bias: Spatially-Aligned Channel Concatenation (U-Net). The U-Net architecture, exemplified by Stable Diffusion [Rombach et al. 2022] and the original U-Net [Ronneberger et al. 2015], is built upon the inductive biases of translation invariance and local connectivity. These models excel at processing data where spatial relationships are strictly preserved across layers. To align with this structural prior, we adopt an explicit conditioning strategy following the InstructPix2Pix [Brooks et al. 2023] paradigm: we treat the reference source image as an extension of the latent input itself. Specifically, the source image I is encoded into the latent space and concatenated with the noisy latent z_t along the channel dimension:

$$c_t = \mathcal{E}(I) \in \mathbb{R}^{h \times w \times d_I}, \quad (2)$$

$$\tilde{z}_t = \text{Concat}(z_t, c_t) \in \mathbb{R}^{h \times w \times (d_z + d_I)}, \quad (3)$$

where \mathcal{E} denotes the VAE encoder. By widening the first convolutional layer to accept $(d_z + d_I)$ channels, we enforce a strict **pixel-to-pixel spatial correspondence**. This allows the convolutional filters to jointly process the noisy target and the clean source structure within the same local receptive field, thereby effectively preserving the high-frequency geospatial details (e.g., road networks, building footprints) essential for RS analysis.

Sequence Bias: In-Context Token Concatenation (DiT). In contrast, Diffusion Transformers (DiTs), such as PixArt- α [Chen et al. 2024], represent a paradigm shift from local processing to global context modeling. DiTs treat images as sequences of flattened patches (tokens), relying on self-attention mechanisms to capture long-range dependencies. For such architectures, naive channel concatenation is sub-optimal as it alters the intrinsic embedding logic of the patches. Instead, we draw inspiration from the emerging capabilities of In-Context Learning in visual generation [Tan et al. 2025a,b]. We propose a **token-level conditioning** strategy that treats the editing task as a sequence completion problem. We encode the source image into a sequence of visual tokens V using the VAE encoder and patchification [Peebles and Xie 2023]:

$$V = \text{Patchify}(\mathcal{E}(I)) \in \mathbb{R}^{n_v \times d}. \quad (4)$$

Then, we append them strictly as a prefix or context to the noisy latent tokens $Z_t \in \mathbb{R}^{n_z \times d}$:

$$\tilde{Z}_t = [V; Z_t] \in \mathbb{R}^{(n_v + n_z) \times d}. \quad (5)$$

This approach leverages the self-attention mechanism to naturally “route” semantic and structural information from the reference tokens V to the generated tokens Z_t . Crucially, this method requires no modification to the internal attention layers or weight structures, preserving the pre-trained generative priors of the DiT backbone while enabling precise, attention-driven edits.

3.3 Implementation Details

Architectures. We use Stable Diffusion v2.1 and v1.5 for U-Net backbones¹ and PixArt- α for DiT backbones. We fine-tune only the image-generation backbones (U-Net or transformer blocks), keeping the VAE and text encoders fixed. Additional architectural details are deferred to the Appendix.

Training Data. We train on the RSCC dataset (Remote Sensing Change Captioning) with over 60,000 bi-temporal satellite image pairs and rich change descriptions [Chen et al. 2025c]. Compared with prior captioning datasets (e.g., LEVIR-CC [Liu et al. 2022], Second-CC [Karaca et al. 2025]) that provide templated one-line

¹The base model checkpoints for Stable Diffusion v1.5 and v2.1 were taken down by Stability AI from Hugging Face in November 2025. We utilized these checkpoints prior to their removal. For researchers wishing to replicate our results, these checkpoints remain available on ModelScope (modelscope.ai).

captions, RSCC supplies semantically rich narratives that capture complex transitions such as construction stages, seasonal phenology, and disaster effects.

Training Setup. All models are trained at 512×512 resolution with the Prodigy optimizer [Mishchenko and Defazio 2024]. Following InstructPix2Pix, we randomly drop the image condition and text condition with probability 0.05 during training to enable classifier-free guidance (unconditional sampling) during inference. We train all models for 30,000 steps on NVIDIA A100 (40GB) GPUs with a global batch size of 32. Additional hyperparameters and optimization details are provided in the Appendix.

4 Results

4.1 Experimental Setup

Baselines. We evaluate against both general-domain and remote-sensing specialized editors. For general domain, we use **Instruct-Pix2Pix** [Brooks et al. 2023], **MagicBrush** [Zhang et al. 2023a], **UltraEdit** [Zhao et al. 2024a], and **Flux-1-Kontext** [Black Forest Labs 2025]. For remote sensing, we use **Text2Earth** (with SDEdit [Meng et al. 2022] for conditioning). Additionally, we use SDEdit with Stable Diffusion backbones v1.5 and v2.1 as a baseline for conditioning. Details of inference hyperparameters are provided in the Appendix.

Evaluation Metrics.

4.2 Change Detection Metric Details

We evaluate the quality of generated post-disaster images using a change detection proxy task. Specifically, we employ a pre-trained ChangeStar model [Zheng et al. 2021a] pre-trained on the Changen2 dataset [Zheng et al. 2024a] and fine-tuned on the xBD dataset [Gupta et al. 2019] (using a specialized checkpoint²) to predict building damage segmentation masks from pre-/post-disaster image pairs. The predicted masks are then compared against ground truth annotations using pixel-wise F1 scores across four damage classes: no-damage, minor-damage, major-damage, and destroyed.

Per-Class F1 Score. For each damage class $c \in \{1, 2, 3, 4\}$, we compute the F1 score as the harmonic mean of precision and recall:

$$F1_c = \frac{2 \cdot TP_c}{2 \cdot TP_c + FP_c + FN_c} \quad (6)$$

where TP_c , FP_c , and FN_c denote true positives, false positives, and false negatives for class c , respectively. Following the xView2 challenge protocol, evaluation is performed only on pixels within ground truth building regions.

Aggregate Damage F1. For aggregate evaluation across all damage classes, we report two metrics:

(1) **Harmonic Mean F1** (standard xView2 metric):

$$F1_{\text{harmonic}} = \frac{4}{\sum_{c=1}^4 (F1_c + \epsilon)^{-1}} \quad (7)$$

where $\epsilon = 10^{-6}$ prevents division by zero. This metric is strict and approaches zero when any individual class has poor performance.

²https://huggingface.co/EVER-Z/Changen2-ChangeStar1x256/blob/main/s0_init_xView2_ft_slc5_cstar_vitb_1x256.pth

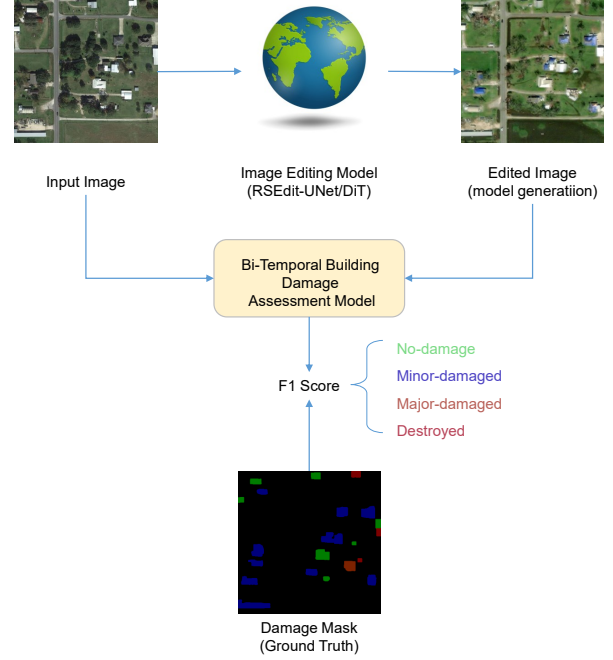


Figure 3: Proposed change-centric evaluation metric using building damage assessment. We leverage a pre-trained ChangeStar model to produce semantic masks for the edited image and compare them to ground-truth damage masks to quantify editing accuracy.

(2) **Weighted F1** (pixel-weighted average):

$$F1_{\text{weighted}} = \frac{\sum_{c=1}^4 F1_c \cdot N_c}{\sum_{c=1}^4 N_c} \quad (8)$$

where N_c denotes the number of ground truth pixels belonging to class c . This metric emphasizes performance on dominant damage classes and is more robust for small sample sizes.

For the full test set evaluation (338 samples), we report $F1_{\text{harmonic}}$ following the xView2 challenge convention. For per-sample visualization and qualitative analysis, we additionally report $F1_{\text{weighted}}$ as it better reflects visual correspondence when not all damage classes are present in individual samples.

Instruction Faithfulness. We report a VLM-based **VIE Score** [Ku et al. 2024] for instruction faithfulness and image quality. The VIE Score is computed as the geometric mean of Semantic Consistency (SC) and Perceptual Quality (PQ), both rated on a scale of 0-10 by a VLM:

$$VIE = \sqrt{SC \times PQ} \quad (9)$$

Conventional proxy metrics showed weak correlation with perceived RS editing quality and are omitted.

4.3 Qualitative Results

We present a visual comparison of **RSEdit** against state-of-the-art general-domain instruction-based image editors in Figure 4. The figure showcases the model’s performance across three distinct

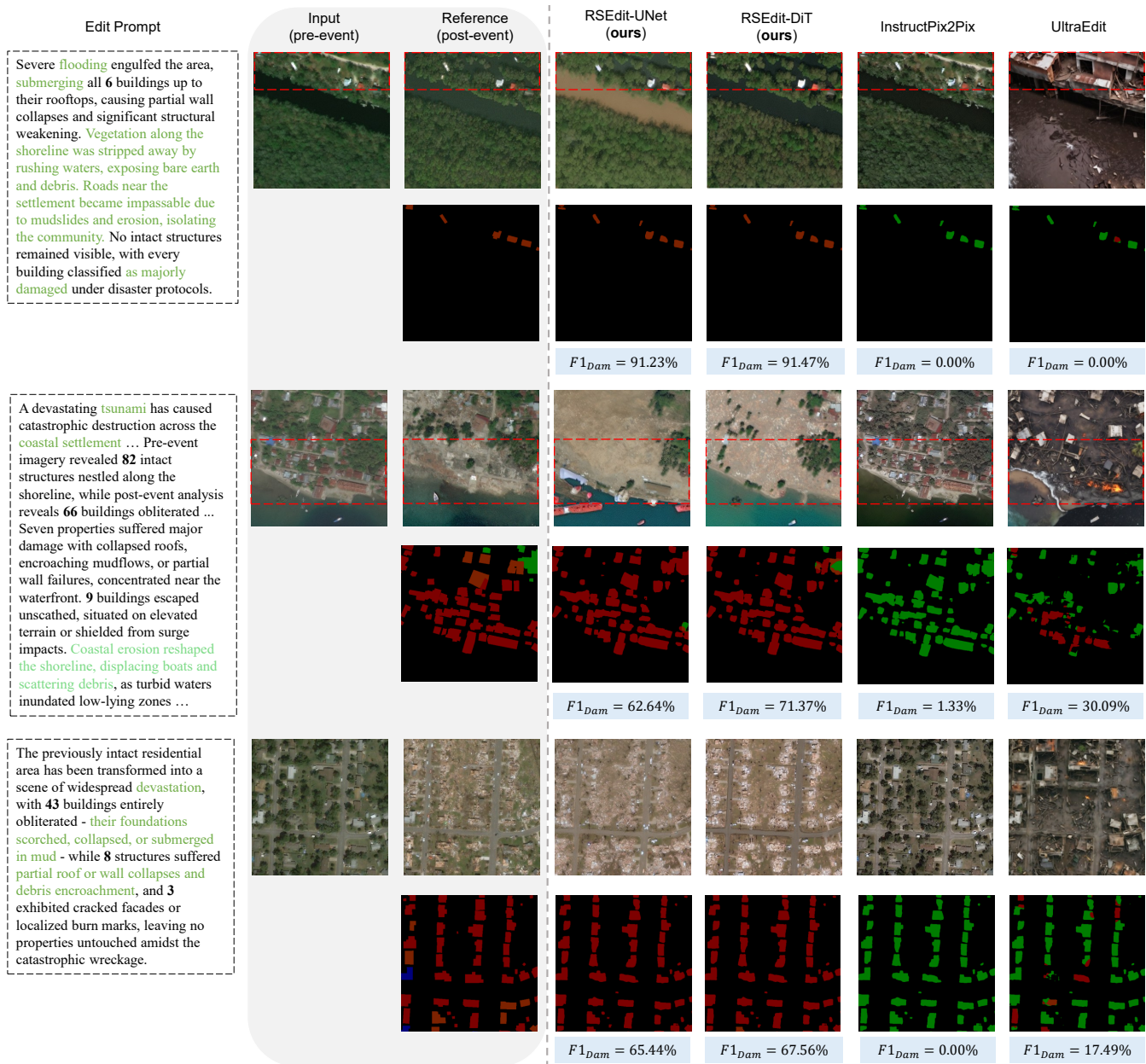


Figure 4: Qualitative comparison of RSEdit against general-domain baselines on disaster simulation scenarios. Columns show, from left to right: Edit Prompt, Input (pre-event), Reference (post-event), RSEdit-UNet (Ours), RSEdit-DiT (Ours), InstructPix2Pix, and UltraEdit. RSEdit variants realistically simulate disaster impacts with high quantitative accuracy (e.g., in Storm: RSEdit-UNet 91.23% $F1_{Dam}$, RSEdit-DiT 91.47%, vs. InstructPix2Pix 0%), whereas baselines fail to follow instructions or introduce artifacts. Noted: $F1_{Dam}$ refers to $F1_{weighted}$ here.

disaster simulation scenarios: Storm (Hurricane Florence 2018), Tsunami (Indonesia Palu Tsunami 2018), and Tornado (Japan Tornado 2011).

RSEdit demonstrates a superior ability to interpret complex geospatial instructions and synthesize physically plausible changes. In the flooding scenario (top row), our model accurately

identifies and inundates low-lying regions, realistically submerging roads and open fields while respecting the elevation logic implied by building footprints. In the tsunami simulation (middle row), RSEdit generates coherent coastal damage patterns, effectively removing structures in the impact zone while maintaining the structural integrity of inland areas. This contrasts sharply

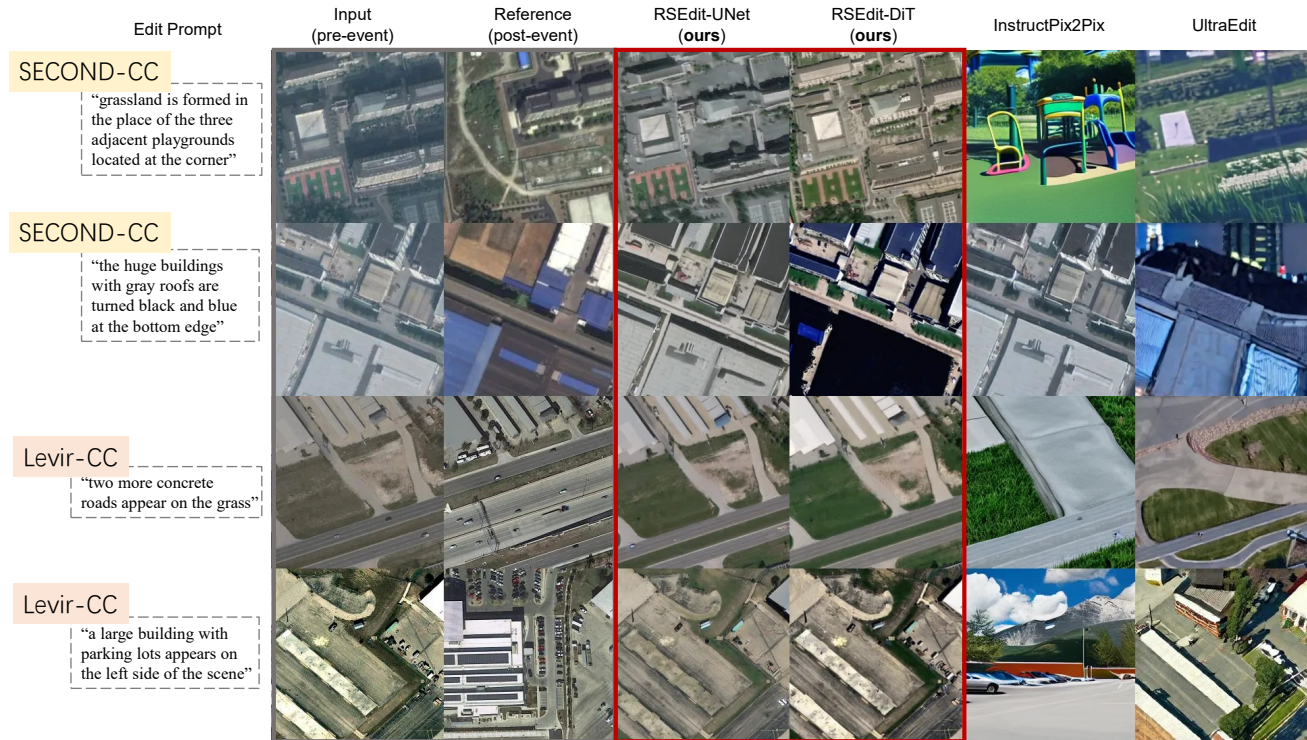


Figure 5: Qualitative results on SECOND-CC and LEVIR-CC benchmarks for out-of-domain generalization. Columns show, from left to right: Edit Prompt, Input (pre-event), Reference (post-event), RSEdit-UNet (Ours), RSEdit-DiT (Ours), Instruct-Pix2Pix, and UltraEdit. Our model trained on RSCC generalizes well to unseen benchmarks without fine-tuning, accurately following complex change descriptions while maintaining geospatial coherence.

with the baseline methods: InstructPix2Pix often exhibits "under-editing," failing to generate significant structural changes, while UltraEdit tends to "over-edit," introducing hallucinations or perspective distortions that break the orthographic constraint of satellite imagery.

Crucially, our method maintains the geospatial coherence of unedited regions—a fundamental requirement for trusted remote sensing analysis. As seen in the building destruction example (bottom row), RSEdit removes roof textures and flattens structures as requested, yet strictly preserves the surrounding road network and vegetation. This selective editing capability validates our architecture-aware adaptation strategy, which leverages the pre-trained priors of diffusion models while enforcing domain-specific constraints through the RSCC dataset.

4.4 Quantitative Evaluation

We quantitatively validate the performance of RSEdit on the RSCC test set³, with results summarized in Table 1. We employ a dual-metric evaluation strategy: the change-centric $F1_{\text{dam}}$ score for semantic accuracy in damage simulation, and the **VIE Score** for assessing instruction faithfulness and visual fidelity.

³We re-split the original RSCC training and testing set by sampling 300 images across both EBD and XBD subsets, as the original test set (1,000 samples) was too large and focused heavily on XBD.

Table 1: Change detection evaluation results. $F1_{\text{dam}}$ denotes the harmonic mean of per-class F1 scores following xView2 protocol. Bold indicates best results, underline indicates second best.

Method	$F1_{\text{dam}} \uparrow$	VIE Scores \uparrow		
		SC	PQ	VIE _{overall}
SD 1.5 [†]	6.87	3.332	2.457	2.492
SD 2.1 [†]	6.05	2.958	2.042	2.120
Text2Earth [†]	5.06	3.970	3.494	3.229
InstructPix2Pix	8.37	4.462	3.195	3.153
MagicBrush	0.96	2.205	2.006	1.638
UltraEdit	1.16	4.250	2.098	2.531
Flux.1-Kontext	5.41	5.065	4.047	3.693
RSEdit_{U-Net}	34.11	5.793	3.657	<u>4.129</u>
RSEdit_{DiT}	25.94	<u>5.759</u>	<u>4.024</u>	4.210

Damage Assessment Accuracy. On the task of semantic change generation, RSEdit establishes a new state-of-the-art. RSEdit_{U-Net} achieves an $F1_{\text{dam}}$ score of 34.11, surpassing the strongest general-domain baseline, InstructPix2Pix (8.37), by a wide margin. This result confirms that general-domain models, despite their photorealism, lack the requisite "world knowledge" to

simulate specific remote sensing phenomena like building damage. Our model, by contrast, correctly synthesizes the visual signatures of damage (e.g., debris, collapsed roofs) that are recognizable by a specialized change detection network.

Perceptual Quality and Faithfulness. The VIE metrics further underscore the robustness of our approach. **RSEdit_{U-Net}** achieves the highest Semantic Consistency (SC) score (5.793), indicating precise adherence to user instructions. **RSEdit_{DiT}** excels in Perceptual Quality (PQ), achieving a score of 4.024, which suggests that the Transformer-based backbone offers superior texture generation capabilities. Both variants outperform the baselines in the overall VIE score, striking an optimal balance between following instructions and maintaining the visual distribution of satellite imagery. The significant performance gap compared to MagicBrush and UltraEdit highlights the necessity of domain-specific fine-tuning for remote sensing tasks.

4.5 Ablation Studies

We evaluate the contribution of the text encoder to our framework’s performance in Table 2. Standard encoders like OpenAI CLIP often struggle with the dense, technical jargon of remote sensing prompts. By replacing the generic encoder with DGTRS-CLIP [Chen et al. 2025a] (a long-context RS-CLIP variant), we observe a substantial improvement in $F1_{\text{dam}}$, rising from 25.62 to 34.11. This gain validates that domain-specific text embedding spaces are crucial for grounding complex instructions. While RemoteCLIP and Git-CLIP offer improvements over the baseline, they fall short of DGTRS-CLIP, likely due to the latter’s ability to handle longer prompts (248 tokens) compared to the standard 77 tokens.

Table 2: Ablation study on text encoders for the RSCC (RSEdit-Split) test set.

Text Encoder	Max Tokens	Dim	$F1_{\text{dam}} \uparrow$	VIE Scores \uparrow	
				SC	PQ
RemoteCLIP	77	768	14.09	5.728	3.737
OpenAI CLIP	77	768	25.62	5.745	3.662
Git-CLIP	77	1024	33.68	5.320	3.713
DGTRS-CLIP	248	768	34.11	5.793	3.657

4.6 Domain Generalization

To assess the robustness of **RSEdit** beyond its training distribution, we evaluate its zero-shot performance on the LEVIR-CC and SECOND-CC benchmarks (Table 3 and Figure 5). Despite being trained exclusively on RSCC, our models generalize effectively to these unseen datasets. On LEVIR-CC, **RSEdit_{DiT}** achieves a VIE score of 2.82, outperforming the instruction-tuned baseline InstructPix2Pix (2.71). Qualitative inspection reveals that **RSEdit** correctly interprets the distinct visual styles of these datasets—handling the different resolution and spectral characteristics of LEVIR-CC without fine-tuning. This generalization capability suggests that **RSEdit** learns a fundamental representation of remote sensing changes rather than overfitting to the specific aesthetics of the source dataset.

Table 3: Out-of-domain generalization on LEVIR-CC [Liu et al. 2022] and SECOND-CC [Karaca et al. 2025] test sets. Our model trained on RSCC generalizes well to unseen benchmarks without fine-tuning.

Method	SC \uparrow	PQ \uparrow	VIE \uparrow
<i>LEVIR-CC</i>			
InstructPix2Pix	4.98	2.33	2.71
UltraEdit	2.45	1.28	1.18
RSEdit_{U-Net}	<u>3.88</u>	<u>3.97</u>	<u>2.74</u>
RSEdit_{DiT}	3.85	4.41	2.82
<i>SECOND-CC</i>			
InstructPix2Pix	3.94	1.87	1.96
UltraEdit	3.69	1.17	1.57
RSEdit_{U-Net}	<u>4.28</u>	<u>2.67</u>	<u>2.61</u>
RSEdit_{DiT}	4.60	3.00	2.91

5 Conclusion and Future Work

We have introduced **RSEdit**, the first unified framework designed to bridge the gap between state-of-the-art generative editing and the specialized domain of remote sensing. By proposing architecture-aware adaptation strategies—channel concatenation for U-Nets and in-context token concatenation for DiTs—we successfully converted pre-trained foundation models into powerful, instruction-following editors. Training on the large-scale RSCC dataset enabled our models to capture the unique spectral, spatial, and physical characteristics of satellite imagery.

Our extensive experiments demonstrate that **RSEdit** significantly outperforms off-the-shelf commercial editing tools, generating physically plausible edits for complex scenarios such as flooding and urban construction while preserving the integrity of the original geospatial data. We believe **RSEdit** paves the way for a new generation of AI-assisted remote sensing tools, offering robust capabilities for data augmentation, environmental simulation, and interactive geospatial analysis.

Future Work. We outline a roadmap to extend **RSEdit** along four directions. *Training Objective:* Beyond the simplified diffusion loss [Ho et al. 2020], we will explore auxiliary objectives (e.g., DINO or CLIP-based) to better align semantics. *Post-Training & Test-Time Scaling:* We plan to evaluate reinforcement-learning alignment methods [Black et al. 2023; Fan et al. 2023; Ge et al. 2025; Liu et al. 2025d; Wallace et al. 2024; Zhu et al. 2024] and inference-time scaling techniques [Ma et al. 2025; Xu et al. 2025; Zhou et al. 2025]. *Data Pruning:* We will investigate pruning strategies to improve training efficiency [Wei et al. 2025; Xia et al. 2023]. *Scaling:* We will study larger models and datasets to further enhance performance.

References

- Bruno Adriano, Naoto Yokoya, Junshi Xia, Hiroyuki Miura, Wen Liu, Masashi Matsuoka, and Shunichi Koshimura. 2021. Learning from Multimodal and Multitemporal Earth Observation Data for Building Damage Mapping. *ISPRS Journal of Photogrammetry and Remote Sensing* 175 (May 2021), 132–143. doi:10.1016/j.isprsjprs.2021.02.016
- Kevin Black, Michael Janner, Yilun Du, Ilya Kostrikov, and Sergey Levine. 2023. Training Diffusion Models with Reinforcement Learning. In *The Twelfth International Conference on Learning Representations*.

- Black Forest Labs. 2025. FLUX.1 Kontext: Flow Matching for In-Context Image Generation and Editing in Latent Space. arXiv:2506.15742 [cs] doi:10.48550/arXiv.2506.15742
- Tim Brooks, Aleksander Holynski, and Alexei A Efros. 2023. Instructpix2pix: Learning to follow image editing instructions. In *Proceedings of the IEEE/CVF Conference on Computer Vision and Pattern Recognition*. 18392–18402.
- Pu Cao, Feng Zhou, Qing Song, and Lu Yang. 2025. Controllable Generation with Text-to-Image Diffusion Models: A Survey. *IEEE Transactions on Pattern Analysis and Machine Intelligence* (2025), 1–20. doi:10.1109/TPAMI.2025.3646548
- Hongruixuan Chen, Jian Song, Olivier Dietrich, Clifford Broni-Bediako, Weihao Xuan, Junjue Wang, Xinlei Shao, Yimin Wei, Junshi Xia, Culing Lan, Konrad Schindler, and Naoto Yokoya. 2025b. BRIGHT: A Globally Distributed Multimodal Building Damage Assessment Dataset with Very-High-Resolution for All-Weather Disaster Response. *Earth System Science Data* 17, 11 (Nov. 2025), 6217–6253. doi:10.5194/essd-17-6217-2025
- Junsong Chen, Jincheng Yu, Chongjian Ge, Lewei Yao, Enze Xie, Zhongdao Wang, James Kwok, Ping Luo, Huchuan Lu, and Zhenguo Li. 2024. PixArt- α : Fast Training of Diffusion Transformer for Photorealistic Text-to-Image Synthesis. In *The Twelfth International Conference on Learning Representations*.
- Weizhi Chen, Yupeng Deng, Wei Jin, Jingbo Chen, Jiansheng Chen, Yuman Feng, Zhihao Xi, Diyou Liu, Kai Li, and Yu Meng. 2025a. DGTRSD and DGTRSClip: A Dual-Granularity Remote Sensing Image–Text Dataset and Vision–Language Foundation Model for Alignment. *IEEE Journal of Selected Topics in Applied Earth Observations and Remote Sensing* 18 (2025), 29113–29130. doi:10.1109/JSTARS.2025.3625958
- Zhenyuan Chen, Chenxi Wang, Ningyu Zhang, and Feng Zhang. 2025c. RSSC: A Large-Scale Remote Sensing Change Caption Dataset for Disaster Events. In *The Thirty-ninth Annual Conference on Neural Information Processing Systems Datasets and Benchmarks Track*.
- Gordon Christie, Neil Fendley, James Wilson, and Ryan Mukherjee. 2018. Functional Map of the World. In *Proceedings of the IEEE Conference on Computer Vision and Pattern Recognition*. 6172–6180.
- Yezhen Cong, Samar Khanna, Chenlin Meng, Patrick Liu, Erik Rozi, Yutong He, Marshall Burke, David B. Lobell, and Stefano Ermon. 2022. Functional Map of the World - Sentinel-2 Corresponding Images. (2022). doi:10.25740/vg497cb6002
- Runmin Dong, Shuai Yuan, Litong Feng, Jinxiao Zhang, Weijia Li, Mengxuan Chen, Bin Luo, Wayne Zhang, and Haohuan Fu. 2026. Transferable Image Synthesis for Remote Sensing Semantic Segmentation via Joint Reference-Semantic Fusion. *Information Fusion* 127 (March 2026), 103839. doi:10.1016/j.inffus.2025.103839
- Ying Fan, Olivia Watkins, Yuqing Du, Hao Liu, Moonkyung Ryu, Craig Boutilier, Pieter Abbeel, Mohammad Ghavamzadeh, Kangwook Lee, and Kimin Lee. 2023. DPQK: Reinforcement Learning for Fine-tuning Text-to-Image Diffusion Models. In *Neural Information Processing Systems*, Vol. 36. Curran Associates, Inc., 79858–79885.
- Lin Geng Foo, Hossein Rahmani, and Jun Liu. 2025. AI-Generated Content (AIGC) for Various Data Modalities: A Survey. *ACM Comput. Surv.* 57, 9 (May 2025), 243:1–243:66. doi:10.1145/3728633
- Shiran Ge, Chenyi Huang, Yang Ai, Qihang Fan, Huaibo Huang, and Ran He. 2025. Expand and Prune: Maximizing Trajectory Diversity for Effective GRPO in Generative Models. arXiv:2512.15347 [cs] doi:10.48550/arXiv.2512.15347
- Ritwik Gupta, Bryce Goodman, Nirav Patel, Ricky Hosfelt, Sandra Sajeev, Eric Heim, Jigar Doshi, Keane Lucas, Howie Choset, and Matthew Gaston. 2019. Creating xBD: A Dataset for Assessing Building Damage from Satellite Imagery. In *Proceedings of the IEEE/CVF Conference on Computer Vision and Pattern Recognition Workshops*. 10–17.
- Fangzhou Han, Lingyu Si, Hongwei Dong, Zhizhuo Jiang, Lamei Zhang, Hao Chen, Yu Liu, and Bo Du. 2025. Exploring Text-Guided Single Image Editing for Remote Sensing Images. *IEEE Journal of Selected Topics in Applied Earth Observations and Remote Sensing* (2025), 18117–18133. doi:10.1109/JSTARS.2025.3584418
- Jonathan Ho, Ajay Jain, and Pieter Abbeel. 2020. Denoising Diffusion Probabilistic Models. In *Advances in Neural Information Processing Systems*. 6840–6851.
- Jonathan Ho, Chitwan Saharia, William Chan, David J. Fleet, Mohammad Norouzi, and Tim Salimans. 2022. Cascaded Diffusion Models for High Fidelity Image Generation. *JMLR* 2022 23, 1 (Jan. 2022), 47:2249–47:2281.
- Yi Huang, Jiancheng Huang, Yifan Liu, Mingfu Yan, Jiayi Lv, Jianzhuang Liu, Wei Xiong, He Zhang, Liangliang Cao, and Shifeng Chen. 2025. Diffusion Model-Based Image Editing: A Survey. *IEEE Transactions on Pattern Analysis and Machine Intelligence* (2025), 1–27. doi:10.1109/TPAMI.2025.3541625
- Ali Can Karaca, Enes Ozelbas, Saadetin Berber, Orkhan Karimli, Turabi Yildirim, and M. Fatih Amasyali. 2025. Robust Change Captioning in Remote Sensing: SECOND-CC Dataset and MModalCC Framework. *IEEE Journal of Selected Topics in Applied Earth Observations and Remote Sensing* (2025), 1–21. doi:10.1109/JSTARS.2025.3600613
- Samar Khanna, Patrick Liu, Linqi Zhou, Chenlin Meng, Robin Rombach, Marshall Burke, David B. Lobell, and Stefano Ermon. 2024. DiffusionSat: A Generative Foundation Model for Satellite Imagery. In *ICLR*.
- Max Ku, Dongfu Jiang, Cong Wei, Xiang Yue, and Wenhui Chen. 2024. VIEScore: Towards Explainable Metrics for Conditional Image Synthesis Evaluation. In *Proceedings of the 62nd Annual Meeting of the Association for Computational Linguistics (Volume 1: Long Papers)*, Lun-Wei Ku, Andre Martins, and Vivek Srikumar (Eds.). Association for Computational Linguistics, Bangkok, Thailand, 12268–12290. doi:10.18653/v1/2024.acl-long.663
- Chenyang Liu, Keyan Chen, Rui Zhao, Zhengxia Zou, and Zhenwei Shi. 2025a. Text2Earth: Unlocking Text-Driven Remote Sensing Image Generation with a Global-Scale Dataset and a Foundation Model. *IEEE Geoscience and Remote Sensing Magazine* (2025), 2–23. doi:10.1109/MGRS.2025.3560455
- Chenyang Liu, Rui Zhao, Hao Chen, Zhengxia Zou, and Zhenwei Shi. 2022. Remote Sensing Image Change Captioning With Dual-Branch Transformers: A New Method and a Large Scale Dataset. *TGRS* (2022), 1–20. doi:10.1109/TGRS.2022.3218921
- Jie Liu, Gongye Liu, Jiajun Liang, Yangguang Li, Jiaheng Liu, Xintao Wang, Pengfei Wan, Di Zhang, and Wanli Ouyang. 2025d. Flow-GRPO: Training Flow Matching Models via Online RL. arXiv:2505.05470 [cs] doi:10.48550/arXiv.2505.05470
- Qiang Liu, Yang Kuang, Jun Yue, Pedram Ghamisi, Weiying Xie, and Leyuan Fang. 2025c. Generating Any Changes in the Noise Domain. *IEEE Transactions on Pattern Analysis and Machine Intelligence* (2025), 1–16. doi:10.1109/TPAMI.2025.3643733
- Shiyu Liu, Yucheng Han, Peng Xing, Fukun Yin, Rui Wang, Wei Cheng, Jiaqi Liao, Yingming Wang, Honghao Fu, Chunrui Han, Guopeng Li, Yuang Peng, Quan Sun, Jingwei Wu, Yan Cai, Zheng Ge, Ranchen Ming, Lei Xia, Xianfang Zeng, Yibo Zhu, Binxing Jiao, Xiangyu Zhang, Gang Yu, and Daxin Jiang. 2025b. StepIX-Edit: A Practical Framework for General Image Editing. arXiv:2504.17761 [cs] doi:10.48550/arXiv.2504.17761
- Nanye Ma, Shangyuan Tong, Haolin Jia, Hexiang Hu, Yu-Chuan Su, Mingda Zhang, Xuan Yang, Yandong Li, Tommi Jaakkola, Xuhui Jia, et al. 2025. Inference-time scaling for diffusion models beyond scaling denoising steps. *arXiv preprint arXiv:2501.09732* (2025).
- Oscar Mañas, Alexandre Lacoste, Xavier Giró-i-Nieto, David Vazquez, and Pau Rodriguez. 2021. Seasonal Contrast: Unsupervised Pre-Training From Uncurated Remote Sensing Data. In *Proceedings of the IEEE/CVF International Conference on Computer Vision*. 9414–9423.
- Chenlin Meng, Yutong He, Yang Song, Jiaming Song, Jiajun Wu, Jun-Yan Zhu, and Stefano Ermon. 2022. SDEdit: Guided Image Synthesis and Editing with Stochastic Differential Equations. In *International Conference on Learning Representations*.
- Konstantin Mishchenko and Aaron Defazio. 2024. Prodigy: An Expediently Adaptive Parameter-Free Learner. In *Proceedings of the 41st International Conference on Machine Learning*. PMLR, 35779–35804.
- Ron Mokady, Amir Hertz, Kfir Aberman, Yael Pritch, and Daniel Cohen-Or. 2023. NULL-text Inversion for Editing Real Images Using Guided Diffusion Models. In *Proceedings of the IEEE/CVF Conference on Computer Vision and Pattern Recognition (CVPR)*. 6038–6047.
- Jiancheng Pan, Shiye Lei, Yuqian Fu, Jiahao Li, Yanxing Liu, Yuze Sun, Xiao He, Long Peng, Xiaomeng Huang, and Bo Zhao. 2025. EarthSynth: Generating Informative Earth Observation with Diffusion Models. arXiv:2505.12108 [cs] doi:10.48550/arXiv.2505.12108
- Li Pang, Xiangyong Cao, Datao Tang, Shuang Xu, Xueru Bai, Feng Zhou, and Deyu Meng. 2026. HSI-Gene: A Foundation Model for Hyperspectral Image Generation. *IEEE Transactions on Pattern Analysis and Machine Intelligence* 48, 1 (Jan. 2026), 730–746. doi:10.1109/TPAMI.2025.3610927
- William Peebles and Saining Xie. 2023. Scalable Diffusion Models with Transformers. In *Proceedings of the IEEE/CVF International Conference on Computer Vision (ICCV)*. 4195–4205.
- Elena Plekhanova, Damien Robert, Johannes Dollinger, Emilia Arens, Philipp Brun, Jan Dirk Wegner, and Niklaus E. Zimmermann. 2025. SSL4Geo: A Global Seasonal Dataset for Geospatial Foundation Models in Ecology. In *Proceedings of the Computer Vision and Pattern Recognition Conference*. 2403–2414.
- Dustin Podell, Zion English, Kyle Lacey, Andreas Blattmann, Tim Dockhorn, Jonas Müller, Joe Penna, and Robin Rombach. 2024. SDXL: Improving Latent Diffusion Models for High-Resolution Image Synthesis. In *The Twelfth International Conference on Learning Representations*.
- Robin Rombach, Andreas Blattmann, Dominik Lorenz, Patrick Esser, and Björn Ommer. 2022. High-Resolution Image Synthesis With Latent Diffusion Models. In *Proceedings of the IEEE/CVF Conference on Computer Vision and Pattern Recognition*. 10684–10695.
- Olaf Ronneberger, Philipp Fischer, and Thomas Brox. 2015. U-Net: Convolutional Networks for Biomedical Image Segmentation. In *International Conference on Medical Image Computing and Computer-Assisted Intervention*, Nassir Navab, Joachim Hornegger, William M. Wells, and Alejandro F. Frangi (Eds.), Vol. 9351. Springer International Publishing, Cham, 234–241. doi:10.1007/978-3-319-24574-4_28
- Srikumar Sastry, Subash Khanal, Aayush Dhakal, and Nathan Jacobs. 2024. GeoSynth: Contextually-Aware High-Resolution Satellite Image Synthesis. In *Proceedings of the IEEE/CVF Conference on Computer Vision and Pattern Recognition*. 460–470.
- Ahmad Sebaq and Mohamed ElHelw. 2024. RSDiff: Remote Sensing Image Generation from Text Using Diffusion Model. *Neural Computing and Applications* 36, 36 (Dec. 2024), 23103–23111. doi:10.1007/s00521-024-10363-3

- Adam Stewart, Nils Lehmann, Isaac Corley, Yi Wang, Yi-Chia Chang, Nassim Ait Ait Ali Braham, Shradha Sehgal, Caleb Robinson, and Arindam Banerjee. 2023. SSL4EO-L: Datasets and Foundation Models for Landsat Imagery. In *Neural Information Processing Systems*, Vol. 36. Curran Associates, Inc., 59787–59807.
- Zhenxiong Tan, Songhua Liu, Xingyi Yang, Qiaochu Xue, and Xinchao Wang. 2025a. OminiControl: Minimal and Universal Control for Diffusion Transformer. In *Proceedings of the IEEE/CVF International Conference on Computer Vision*. 14940–14950.
- Zhenxiong Tan, Qiaochu Xue, Xingyi Yang, Songhua Liu, and Xinchao Wang. 2025b. OminiControl2: Efficient Conditioning for Diffusion Transformers. arXiv:2503.08280 [cs] doi:10.48550/arXiv.2503.08280
- Datao Tang, Xiangyong Cao, Xingsong Hou, Zhongyuan Jiang, Junmin Liu, and Deyu Meng. 2024. CRS-Diff: Controllable Remote Sensing Image Generation With Diffusion Model. *TGRS* (2024), 1–14. doi:10.1109/TGRS.2024.3453414
- Datao Tang, Hao Wang, Yudeng Xin, Hui Qiao, Dongsheng Jiang, Yin Li, Zhiheng Yu, and Xiangyong Cao. 2025. TerraGen: A Unified Multi-Task Layout Generation Framework for Remote Sensing Data Augmentation. arXiv:2510.21391 [cs] doi:10.48550/arXiv.2510.21391
- Aysim Toker, Marvin Eisenberger, Daniel Cremers, and Laura Leal-Taixé. 2024. Sat-Synth: Augmenting Image-Mask Pairs through Diffusion Models for Aerial Semantic Segmentation. In *Proceedings of the IEEE/CVF Conference on Computer Vision and Pattern Recognition (CVPR)*. 27695–27705.
- Bram Wallace, Meihua Dang, Rafael Rafailov, Linqi Zhou, Aaron Lou, Senthil Purushwalkam, Stefano Ermon, Caiming Xiong, Shafiq Joty, and Nikhil Naik. 2024. Diffusion Model Alignment Using Direct Preference Optimization. In *Proceedings of the IEEE/CVF Conference on Computer Vision and Pattern Recognition*. 8228–8238.
- Junjue Wang, Ailong Ma, Zihang Chen, Zhuo Zheng, Yuting Wan, Liangpei Zhang, and Yanfei Zhong. 2024a. EarthVQANet: Multi-task Visual Question Answering for Remote Sensing Image Understanding. *ISPRS Journal of Photogrammetry and Remote Sensing* 212 (June 2024), 422–439. doi:10.1016/j.isprsjprs.2024.05.001
- Junjue Wang, Weihao Xuan, Heli Qi, Zhihao Liu, Kunyi Liu, Yuhan Wu, Hongruixuan Chen, Jian Song, Junshi Xia, Zhuo Zheng, and Naoto Yokoya. 2025. DisasterM3: A Remote Sensing Vision-Language Dataset for Disaster Damage Assessment and Response. In *NeurIPS*.
- Junjue Wang, Zhuo Zheng, Zihang Chen, Ailong Ma, and Yanfei Zhong. 2024c. EarthVQA: Towards Queryable Earth via Relational Reasoning-Based Remote Sensing Visual Question Answering. *Proceedings of the AAAI Conference on Artificial Intelligence* 38, 6 (March 2024), 5481–5489. doi:10.1609/aaai.v38i6.28357
- Junjue Wang, Yanfei Zhong, Zihang Chen, Zhuo Zheng, Ailong Ma, and Liangpei Zhang. 2026. EarthVL: A Progressive Earth Vision-Language Understanding and Generation Framework. arXiv:2601.02783 [cs] doi:10.48550/arXiv.2601.02783
- Mingze Wang, Lili Su, Cilin Yan, Sheng Xu, Pengcheng Yuan, Xiaolong Jiang, and Baochang Zhang. 2024b. RSBuilding: Toward General Remote Sensing Image Building Extraction and Change Detection With Foundation Model. *IEEE Transactions on Geoscience and Remote Sensing* 62 (2024), 1–17. doi:10.1109/TGRS.2024.3439395
- Yi Wang, Nassim Ait Ali Braham, Zhitong Xiong, Chenying Liu, Conrad M. Albrecht, and Xiao Xiang Zhu. 2023. SSL4EO-S12: A Large-Scale Multimodal, Multitemporal Dataset for Self-Supervised Learning in Earth Observation [Software and Data Sets]. *IEEE Geoscience and Remote Sensing Magazine* 11, 3 (Sept. 2023), 98–106. doi:10.1109/MGRS.2023.3281651
- Fan Wei, Runmin Dong, Yushan Lai, Yixiang Yang, Zhaoyang Luo, Jinxiao Zhang, Miao Yang, Shuai Yuan, Jiayao Zhao, Bin Luo, and Haohuan Fu. 2025. RS-Prune: Training-Free Data Pruning at High Ratios for Efficient Remote Sensing Diffusion Foundation Models. arXiv:2512.23239 [cs] doi:10.48550/arXiv.2512.23239
- Xiaobo Xia, Jiale Liu, Jun Yu, Xu Shen, Bo Han, and Tongliang Liu. 2023. Moderate Coreset: A Universal Method of Data Selection for Real-world Data-efficient Deep Learning. In *The Eleventh International Conference on Learning Representations*.
- Katherine Xu, Lingzhi Zhang, and Jianbo Shi. 2025. Good Seed Makes a Good Crop: Discovering Secret Seeds in Text-to-Image Diffusion Models. In *2025 IEEE/CVF Winter Conference on Applications of Computer Vision (WACV)*. 3024–3034. doi:10.1109/WACV61041.2025.00299
- Weihao Xuan, Junjue Wang, Heli Qi, Zihang Chen, Zhuo Zheng, Yanfei Zhong, Junshi Xia, and Naoto Yokoya. 2025. DynamicVL: Benchmarking Multimodal Large Language Models for Dynamic City Understanding. In *NeurIPS*.
- Yunkai Yang, Yudong Zhang, Kunquan Zhang, Jinxiao Zhang, Xinying Chen, Haohuan Fu, and Runmin Dong. 2025. Task-Oriented Data Synthesis and Control-Rectify Sampling for Remote Sensing Semantic Segmentation. arXiv:2512.16740 [cs] doi:10.48550/arXiv.2512.16740
- Srikar Yellapragada, Alexandros Graikos, Kostas Triaridis, Prateek Prasanna, Rajarsi Gupta, Joel Saltz, and Dimitris Samaras. 2025. ZoomLDM: Latent Diffusion Model for Multi-scale Image Generation. In *CVPR*. 23453–23463.
- Qifan Yu, Wei Chow, Zhongqi Yue, Kaihang Pan, Yang Wu, Xiaoyang Wan, Juncheng Li, Siliang Tang, Hanwang Zhang, and Yueting Zhuang. 2025a. Anyedit: Mastering unified high-quality image editing for any idea. In *Proceedings of the Computer Vision and Pattern Recognition Conference*. 26125–26135.
- Zhiping Yu, Chenyang Liu, Liqin Liu, Zhenwei Shi, and Zhengxia Zou. 2025b. MetaEarth: A Generative Foundation Model for Global-Scale Remote Sensing Image Generation. *IEEE Transactions on Pattern Analysis and Machine Intelligence* (March 2025), 1764–1781. doi:10.1109/TPAMI.2024.3507010
- Qi Zang, Jiayi Yang, Shuang Wang, Dong Zhao, Wenjun Yi, and Zhun Zhong. 2025. ChangeDiff: A Multi-Temporal Change Detection Data Generator with Flexible Text Prompts via Diffusion Model. *Proceedings of the AAAI Conference on Artificial Intelligence* 39, 9 (April 2025), 9763–9771. doi:10.1609/aaai.v39i9.33058
- Zheyuan Zhan, Defang Chen, Jian-Ping Mei, Zhenghe Zhao, Jiawei Chen, Chun Chen, Siwei Lyu, and Can Wang. 2025. Conditional Image Synthesis with Diffusion Models: A Survey. *Transactions on Machine Learning Research* (2025).
- Jiawei Zhang, Xiaolin Zhou, Weidong Jiang, Xiaolong Su, Zhen Liu, and Li Liu. 2026. Extrapolate Azimuth Angles: Text and Edge Guided ISAR Image Generation Based on Foundation Model. *ISPRS Journal of Photogrammetry and Remote Sensing* 232 (Feb. 2026), 109–123. doi:10.1016/j.isprsjprs.2025.12.002
- Kai Zhang, Lingbo Mo, Wenhu Chen, Huan Sun, and Yu Su. 2023a. MagicBrush: A Manually Annotated Dataset for Instruction-Guided Image Editing. In *Neural Information Processing Systems*, Vol. 36. Curran Associates, Inc., 31428–31449.
- Kai Zhang, Lingbo Mo, Wenhu Chen, Huan Sun, and Yu Su. 2023b. Magicbrush: A manually annotated dataset for instruction-guided image editing. *Advances in Neural Information Processing Systems* (2023), 31428–31449.
- Lvmin Zhang, Anyi Rao, and Maneesh Agrawala. 2023c. Adding Conditional Control to Text-to-Image Diffusion Models. In *2023 IEEE/CVF International Conference on Computer Vision (ICCV)*. 3813–3824. doi:10.1109/ICCV51070.2023.00355
- Yuanrui Zhang, Liqin Liu, Keyan Chen, Jia Xu, Zhenwei Shi, and Zhengxia Zou. 2025a. Cascaded Autoregressive Diffusion Models for Remote Sensing Scene Generation. *IEEE Transactions on Geoscience and Remote Sensing* (2025), 1–17. doi:10.1109/TGRS.2025.3622225
- Zechuan Zhang, Ji Xie, Yu Lu, Zongxin Yang, and Yi Yang. 2025b. Enabling Instructional Image Editing with In-Context Generation in Large Scale Diffusion Transformer. In *NeurIPS*.
- Haozhe Zhao, Xiaojian Ma, Liang Chen, Shuzheng Si, Rujie Wu, Kaikai An, Peiyu Yu, Minjia Zhang, Qing Li, and Baobao Chang. 2024a. UltraEdit: Instruction-based Fine-Grained Image Editing at Scale. In *The Thirty-eight Conference on Neural Information Processing Systems Datasets and Benchmarks Track*.
- Haozhe Zhao, Xiaojian Shawn Ma, Liang Chen, Shuzheng Si, Rujie Wu, Kaikai An, Peiyu Yu, Minjia Zhang, Qing Li, and Baobao Chang. 2024b. Ultraedit: Instruction-based fine-grained image editing at scale. *Advances in Neural Information Processing Systems* (2024), 3058–3093.
- Zhenghui Zhao, Chen Wu, Di Wang, Hongruixuan Chen, and Zhuo Zheng. 2025. ChangeBridge: Spatiotemporal Image Generation with Multimodal Controls for Remote Sensing. arXiv:2507.04678 [cs] doi:10.48550/arXiv.2507.04678
- Zhuo Zheng, Stefano Ermon, Dongjun Kim, Liangpei Zhang, and Yanfei Zhong. 2024a. ChangeNet2: Multi-Temporal Remote Sensing Generative Change Foundation Model. *IEEE Transactions on Pattern Analysis and Machine Intelligence* (2024), 1–17. doi:10.1109/TPAMI.2024.3475824
- Zhuo Zheng, Ailong Ma, Liangpei Zhang, and Yanfei Zhong. 2021a. Change Is Everywhere: Single-Temporal Supervised Object Change Detection in Remote Sensing Imagery. In *Proceedings of the IEEE/CVF International Conference on Computer Vision*. 15193–15202.
- Zhuo Zheng, Shiqi Tian, Ailong Ma, Liangpei Zhang, and Yanfei Zhong. 2023. Scalable Multi-Temporal Remote Sensing Change Data Generation via Simulating Stochastic Change Process. In *Proceedings of the IEEE/CVF International Conference on Computer Vision*. 21761–21770. doi:10.1109/ICCV51070.2023.01994
- Zhuo Zheng, Yanfei Zhong, Zijing Wan, Liangpei Zhang, and Stefano Ermon. 2025. Neural Disaster Simulation for Transferable Building Damage Assessment. *Remote Sensing of Environment* (Dec. 2025), 114979. doi:10.1016/j.rse.2025.114979
- Zhuo Zheng, Yanfei Zhong, Junjue Wang, Ailong Ma, and Liangpei Zhang. 2021b. Building Damage Assessment for Rapid Disaster Response with a Deep Object-Based Semantic Change Detection Framework: From Natural Disasters to Man-Made Disasters. *Remote Sensing of Environment* (Nov. 2021), 112636. doi:10.1016/j.rse.2021.112636
- Zhuo Zheng, Yanfei Zhong, Liangpei Zhang, Marshall Burke, David B. Lobell, and Stefano Ermon. 2024b. Towards Transferable Building Damage Assessment via Unsupervised Single-Temporal Change Adaptation. *Remote Sensing of Environment* 315 (Dec. 2024), 114416. doi:10.1016/j.rse.2024.114416
- Zikai Zhou, Shitong Shao, Lichen Bai, Shufei Zhang, Zhiqiang Xu, Bo Han, and Zeke Xie. 2025. Golden Noise for Diffusion Models: A Learning Framework. In *ICCV*. 17688–17697.
- Huaisheng Zhu, Teng Xiao, and Vasant G. Honavar. 2024. DSP0: Direct Score Preference Optimization for Diffusion Model Alignment. In *The Thirteenth International Conference on Learning Representations*.

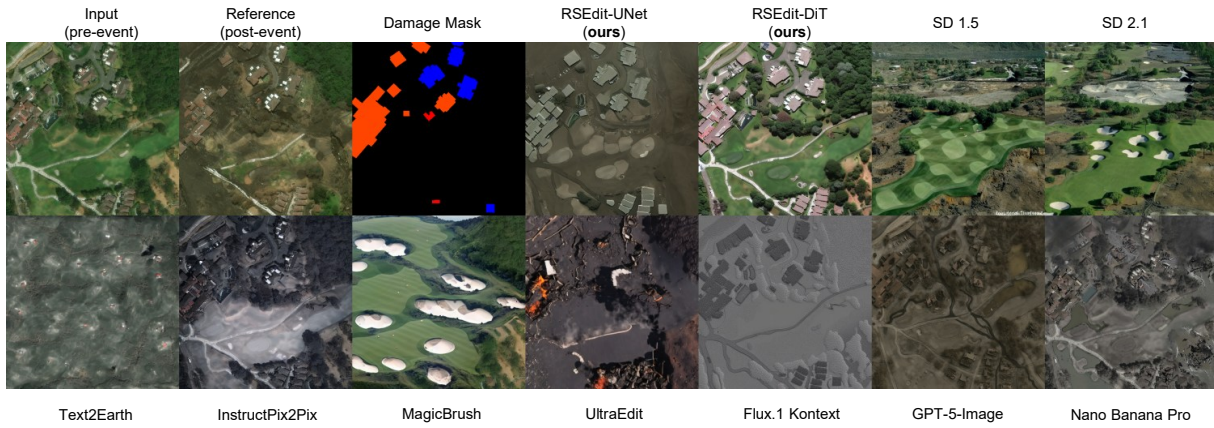


Figure 6: Comparison of qualitative results for the Guatemala Volcano scenario. See full prompt in appendix.

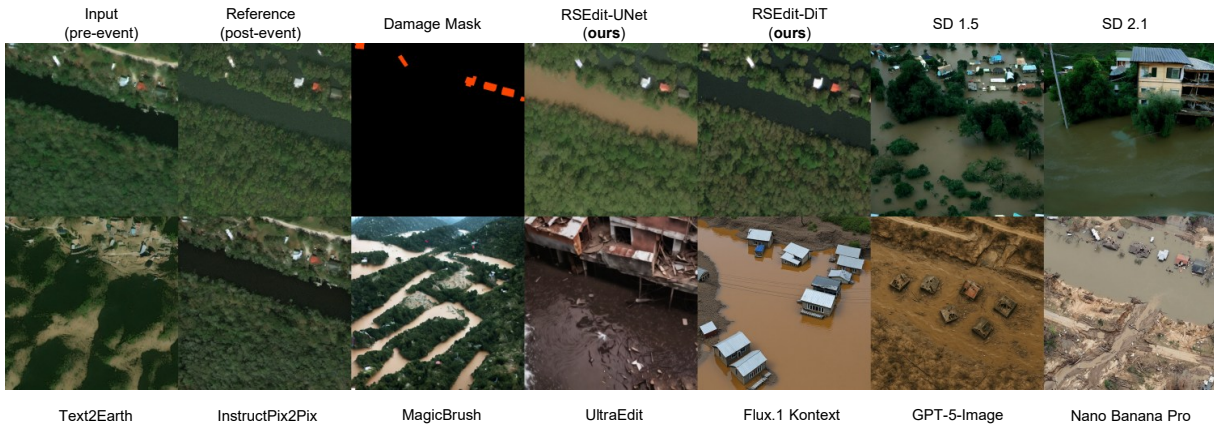


Figure 7: Comparison of qualitative results for the Hurricane Florence scenario. See full prompt in appendix.

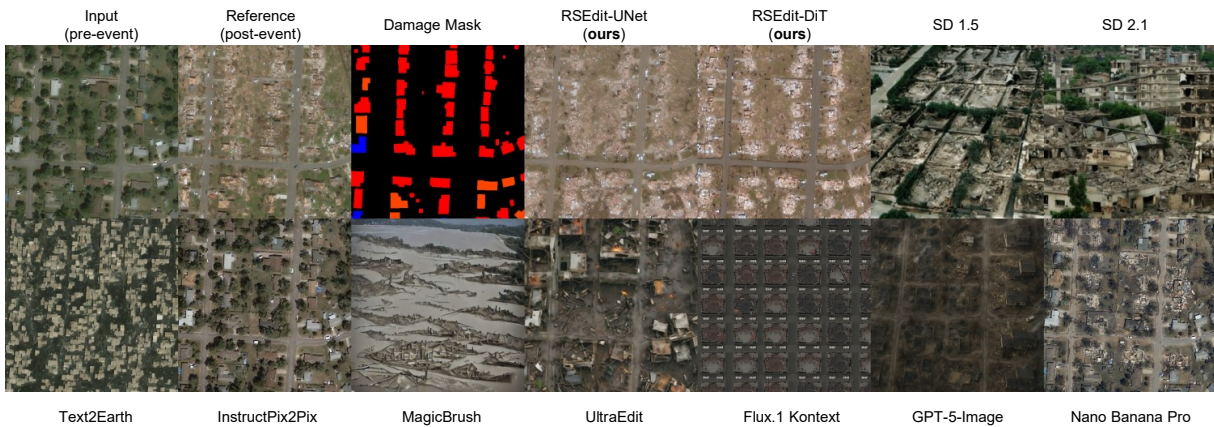


Figure 8: Comparison of qualitative results for the Joplin Tornado scenario. See full prompt in appendix.

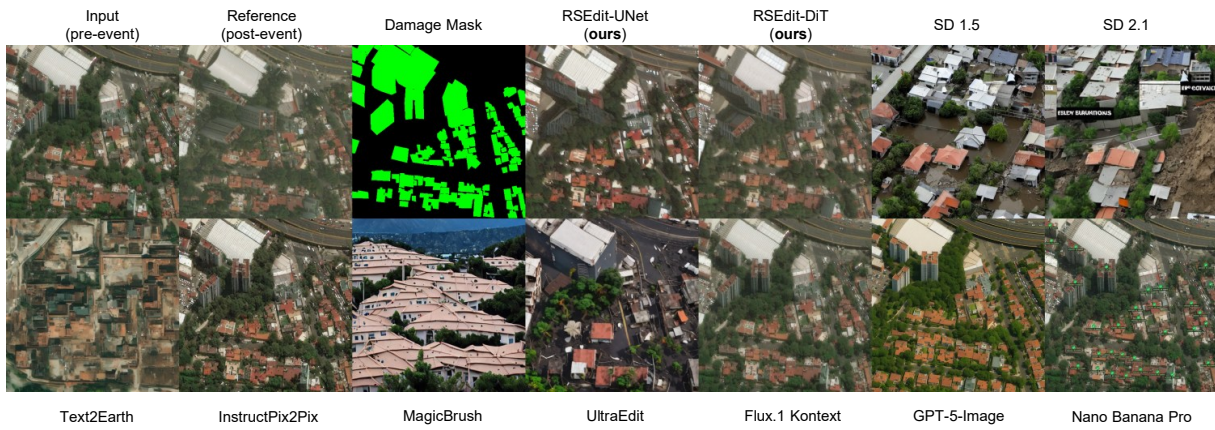


Figure 9: Comparison of qualitative results for the Mexico Earthquake scenario. See full prompt in appendix.

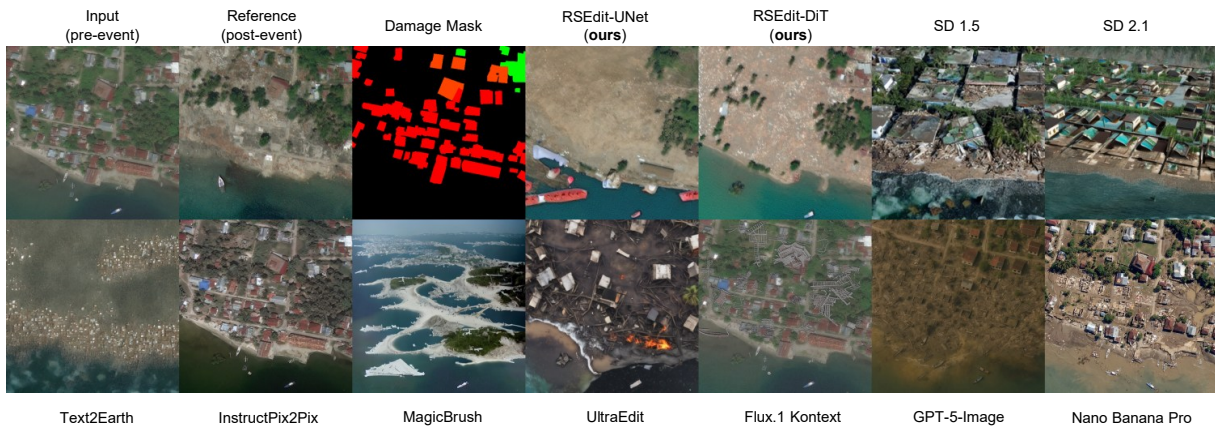


Figure 10: Comparison of qualitative results for the Palu Tsunami scenario. See full prompt in appendix.



Figure 11: Comparison of qualitative results for the Portugal Wildfire scenario. See full prompt in appendix.

A Training Implementation Details

We train two variants of **RSEdit** based on different diffusion architectures: U-Net (Stable Diffusion 1.5) and DiT (PixArt- α). All models are trained on the RSCC dataset using the instruction-following paradigm. Table 4 summarizes the key training hyperparameters.

Table 4: Training hyperparameters for **RSEdit model variants. All models use mixed precision (bfloat16) and Prodigy optimizer.**

Hyperparameter	RSEdit-UNet	RSEdit-DiT
Base Model	SD 1.5	PixArt- α
Resolution	512×512	512×512
Global Batch Size	32	32
Gradient Accumulation	1	4
GPUs	1	4
Per GPU Batch Size	32	2
Optimizer	Prodigy	Prodigy
Learning Rate	1.0	1.0
Weight Decay	0.01	0.01
Training Steps	30,000	30,000
Conditioning Dropout	0.05	0.05
EMA	Yes	Yes
Mixed Precision	bfloat16	bfloat16
Training Time	~16 hours	~16 hours
Hardware	1×A100 (40GB)	4×A100 (40GB)

B Inference Implementation Details

Table 5 presents the inference configurations used in our evaluation. We employ 100 denoising steps for all models to ensure high-quality generation. For SDedit, we set the strength as 0.75.

Table 5: Inference configurations for **RSEdit and baseline models.**

Model	CFG Scale	Img CFG	Scheduler
RSEdit-UNet	7.5	1.5	EulerDiscrete
RSEdit-DiT	7.5	–	DPMSolverMultistep
InstructPix2Pix	7.5	1.5	EulerAncestralDiscrete
MagicBrush	7.5	1.5	PNDM
UltraEdit	7.5	–	FlowMatchEulerDiscrete
Flux.1-Kontext	3.5	–	FlowMatchEulerDiscrete
Text2Earth	4.0	–	EulerDiscrete
SDedit (SD 1.5)	7.5	–	PNDM

C Prompts for Qualitative Samples

Table 6 provides the full text instructions used to generate the results for the samples presented in our qualitative evaluation.

Table 6: Full text instructions for the samples used in qualitative analysis.

Guatemala Volcano

The volcanic eruption transformed the lush golf course into a desolate ash-covered landscape, with once-pristine fairways blanketed in gray debris and expanded water bodies inundating low-lying areas. Five buildings exhibit minor damage, showing partial burns, cracked roofs, and scattered volcanic material, while six structures suffer major collapse, their walls and roofs shattered by encroaching lava flows or mudslides. Two properties are entirely obliterated, reduced to scorched foundations or submerged under torrents of water and sediment, marking a catastrophic shift from pre-event tranquility to post-disaster devastation.

Joplin Tornado

The previously intact residential area has been transformed into a scene of widespread devastation, with 43 buildings entirely obliterated— their foundations scorched, collapsed, or submerged in mud—while 8 structures suffered partial roof or wall collapses and debris encroachment, and 3 exhibited cracked facades or localized burn marks, leaving no properties untouched amidst the catastrophic wreckage.

Portugal Wildfire

Wildfire impacts revealed minor damage to three buildings, showing partial burn marks, scattered debris, and disrupted roofing, while one structure remained undisturbed. Surrounding vegetation exhibited widespread charring, with ash-covered patches and reduced greenery density. Roads displayed residual smoke haze and localized erosion from firefighting water runoff, altering terrain contours near affected sites.

Hurricane Florence

Severe flooding engulfed the area, submerging all six buildings up to their rooftops, causing partial wall collapses and significant structural weakening. Vegetation along the shoreline was stripped away by rushing waters, exposing bare earth and debris. Roads near the settlement became impassable due to mudslides and erosion, isolating the community. No intact structures remained visible, with every building classified as majorly damaged (Level 2) under disaster protocols.

Mexico Earthquake

Post-earthquake assessment shows no structural damage detected in 89 evaluated buildings, with all structures maintaining intact roofs, walls, and foundations. Nearby infrastructure, including roads and vegetation, displays no evidence of collapse, flooding, or volcanic activity. The area visually aligns with pre-disaster conditions, resulting in Disaster Level 0 (No Damage) classification for all inspected properties.

Palu Tsunami

A devastating tsunami has caused catastrophic destruction across the coastal settlement, transforming the landscape from a densely populated area into a scene of widespread ruin. Pre-event imagery revealed 82 intact structures nestled along the shoreline, while post-event analysis reveals 66 buildings obliterated (Disaster Level 3)—scorched, submerged, or entirely erased—leaving only skeletal remains or vacant lots. Seven properties suffered major damage (Level 2), with collapsed roofs, encroaching mudflows, or partial wall failures, concentrated near the waterfront. Nine buildings escaped unscathed (Level 0), situated on elevated terrain or shielded from surge impacts. Coastal erosion reshaped the shoreline, displacing boats and scattering debris, as turbid waters inundated low-lying zones, marking the tsunami's merciless advance.
